Magnetic Colloids from Magnetotactic Bacteria: Chain Formation and Colloidal Stability

Albert P. Philipse* and Diana Maas†

Van't Hoff Laboratory for Physical and Colloid Chemistry, Utrecht University, Debye Institute, Padualaan 8, 3584 CH Utrecht, The Netherlands

Received June 21, 2002. In Final Form: September 10, 2002

Single-domain magnetite (Fe_3O_4) crystals, harvested from magnetotactic bacteria, display on transmission electron micrographs the cluster morphologies (folded chains, flux-closure rings) predicted for magnetic colloids with dominant dipolar attractions. These strong attractions are responsible for the linear magnetite chains inside bacteria but do not affect the colloidal stability of the bacteria, as confirmed by analytic sedimentation experiments. Calculations of the interaction energy between dipole chains show that the magnetic component of the interbacteria interaction is negligible due to screening of dipolar forces: the bacteria sense only the geomagnetic field but not each other's compass.

1. Introduction

A striking property of magnetotactic bacteria such as *Magnetospirillum magnetotacticum*[1] is their ability to orient themselves in the earth magnetic field. Their compass is a chain of magnetite colloids which keeps the long axis of the bacteria parallel to the field direction. Propelled by their flagella, the bacteria migrate in a net downward direction, following the declination of the field lines of the earth, toward oxygen-poor regions with advantages for survival (biogenic magnetite as old as 7×10^8 years has been found;[2] these bacteria indeed survive). Magnetotactic bacteria occur widely in natural sediments from both marine and freshwater habitats. They produce intracellular, membrane-bounded magnetite (Fe_3O_4),[3] greigite (Fe_3S_4),[4] and pyrrhotite (Fe_7S_8) particles.[5] A fairly narrow size distribution of particles of colloidal size and specific crystallographic orientations characterize the mineral particles and their enveloping membrane, together called magnetosomes.

The geomagnetic sensor of the bacteria is also intriguing from a colloid science point of view. Single-domain magnetite colloids[6] in laboratory-made dispersions ("ferrofluids") have diameters in the range of 5−15 nm, considerably smaller than bacterial magnetite (≈50 nm). Magnetic interactions in ferrofluids are fairly weak,[7] and since these interactions increase quadratically with the particle volume, biogenic magnetite colloids are expected to have quite strong dipolar (magnetic) interactions. Thus it would be interesting to harvest the biogenic magnetite and see, for example, whether (outside bacteria) the biomagnetite particles form structures such as chains and even rings. These are predicted for strong dipoles,[8] though as far as we know flux-closure rings have never been observed or imaged in Fe_3O_4 ferrofluids.

Demonstrating the existence of such dipole structures by electron-micrograph imaging was the initial motivation for our work on bacterial magnetite, in addition to evaluating bacterial cultivation as an alternative to the usual inorganic preparation methods of magnetite colloids.[7,9] (These methods are quite restrictive with respect to particle size and shape.) We noticed that the bacteria in our study form quite stable (i.e., nonaggregated) dispersions in water. This followed, for example, from the concentration dependence of the rate at which (dead) bacteria settle in the earth gravitational field. Nevertheless, these bacteria possess long backbones of strongly attractive magnets, so the question arose of why these magnets did not affect the colloidal stability of the bacterial "particles". Our explanation derives from theory[10] and simulations[10,11] in the literature which show that chaining of strong dipoles strongly suppresses further aggregation or phase separation of magnetic colloids.

Although several species of magnetotactic bacteria have been isolated from natural environments, subsequently laboratory culture of most strains is difficult because they are obligate microaerophilic. To our knowledge, nearly all information on culturing of magnetotactic bacteria has been acquired from studies on *M. magnetotacticum*.[12] This organism requires microaerobic conditions and may be grown in a chemically defined medium, as described in section 3. In section 4, we discuss various characterization experiments such as sedimentation and electrophoresis on the cultivated bacterial cells, as well as electron micrographs of structures of magnetic particles released from the cells. Interactions between (and in) the bacterial magnetite chains are discussed in section 4.7. First, some theoretical aspects are treated in section 2.

* Corresponding author.
† Present address: Fuji, Oudenstaart 1, PB 90156, 5000 LJ Tilburg, The Netherlands.

(1) Blakemore, R. P. *Science* **1975**, *190*, 377.
(2) Butler, R. F. *Paleomagnetism*; Blackwell Scientific: Oxford, 1992.
(3) Blakemore, R. P.; Maratea, D.; Wolfe, R. S. *J. Bacteriol.* **1979**, *140* (2), 720.
(4) Bazylinski, D. A.; Heywood, B. R.; Mann, S.; Frankel, R. B. *Nature* **1993**, *366*, 218.
(5) Farina, M.; Esquivel, D. M. S.; Lins de Barros, H. G. P. *Nature* **1990**, *343*, 256.
(6) Rosensweig, R. E. *Ferrohydrodynamics*; Cambridge University Press: Cambridge, 1985.
(7) Ewijk, G. A. van Phase behavior of mixtures of magnetic colloids and nonadsorbing polymer. Thesis, Utrecht University, Utrecht, The Netherlands, 2001.
(8) Jacobs, I. S.; Bean, C. P. In *Magnetism*; Rado, G. T., Suhl, H., Eds.; Academic Press: New York, 1963; Vol. III.
(9) Cabuil, V.; Perzynski, R. In *Magnetic Fluids and Applications Handbook*; Berkovski, B., Ed.; Begell House: New York, 1996.
(10) Halsey, T. C.; Toor, W. *J. Stat. Phys.* **1990**, *61*, 1257. G. J. Vroege and B. J. de Gans (unpublished results) pointed out to us that this reference contains an error: eq 15 is their corrected version for the result in ref 10.
(11) Teixeira, P. I. C.; Tavares, J. M.; Telo da Gama, M. M. *J. Phys.: Condens. Matter* **2000**, *12*, R411−R434.
(12) Blakemore, R. P.; Blakemore, N. A.; Bazylinski, D. A.; Moench, T. T. *Bergey's Manual of Systematic Bacteriology*; Williams & Wilkins: Baltimore, 1989.

10.1021/la0205811 CCC: $22.00
Published on Web 11/07/2002

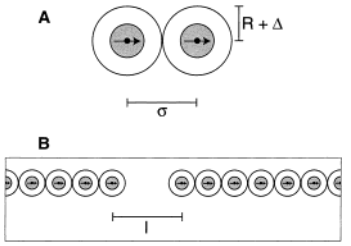

Figure 1. (A) Two dipoles embedded in a sphere of radius R in a head-to-tail configuration with maximal attraction energy. A nonmagnetic shell thickness Δ reduces the energy at contact distance σ. (B) Two ends of rigid dipole chains with an interaction given by eq 9.

2. Chains of Magnetic Colloids

We start with recapitulating some equations pertinent for (chains of) single-domain magnetic colloids. Suppose two magnetic dipoles with orientation unit vectors $\hat{\mathbf{s}}_1$ and $\hat{\mathbf{s}}_2$, separated by a center-to-center distance r along the unit vector $\hat{\mathbf{r}}$, are embedded in a solid magnetite particle, covered with an organic (lipid) coating, which allows a closest approach of the dipole centers to a distance $r = \sigma$. The interaction energy for the two dipoles is in units of the thermal energy kT:

$$V/kT = \lambda(\sigma/r)^3[\hat{\mathbf{s}}_1\cdot\hat{\mathbf{s}}_2 - 3(\hat{\mathbf{s}}_1\cdot\hat{\mathbf{r}})(\hat{\mathbf{s}}_2\cdot\hat{\mathbf{r}})] \tag{1}$$

The parameter λ measures the contact energy at $r = \sigma$:

$$\lambda = \mu_0\mu^2/4\pi kT\sigma^3 \tag{2}$$

where μ_0 is the free-space permeability and μ is the particle magnetic moment. For a fully saturated (single-domain) particle of volume v_p,

$$\mu = v_p m_s \tag{3}$$

with m_s being the saturation magnetization of the bulk material. For magnetic spheres with radius R and a nonmagnetic coating of thickness Δ (Figure 1), the distance of closest approach is $\sigma = 2R + 2\Delta$. Hence,

$$\lambda = \frac{\mu_0 {m_s}^2 \pi}{18kT}\frac{R^3}{(1 + \Delta/R)^3} \tag{4}$$

The maximal attraction for two dipoles occurs at a head-to-tail configuration (Figure 1):

$$V_{max}/kT = -2\lambda \qquad \text{for } r = \sigma \tag{5}$$

For a collection of dipoles, it is energetically favorable to form linear chains of dipoles; the energy gain to add one dipole to the end of a long linear chain is[13]

$$V/kT = -2\lambda\sum_{n=1}^{\infty}(1/n^3) \approx -2\lambda(1.202) \tag{6}$$

as follows from eq 1; n labels the dipoles in the chain. For magnetotactic bacteria, it is also interesting to know the energy gain for the fusion of two chains and, more in general, the attraction between chain ends at some finite distance. This attraction can be evaluated as follows. Consider a long, straight dipole chain with its head-sphere a distance l removed from the center of the tail-sphere of another chain, the two rigid chains being in one line with their main axes (see Figure 1B). The interaction energy between two dipoles from different chains is (see eq 1)

$$\frac{V_{n,m}}{kT} = -2\lambda\left(\frac{\sigma}{l + n\sigma + m\sigma}\right)^3 \tag{7}$$

in which σ is the distance between neighbor centers in a chain; dipoles are numbered as $n,m = 0,1,2$ .... The total interaction energy is therefore

$$\frac{V}{kT} = \frac{1}{kT}\sum_{n=0}^{\infty}\sum_{m=0}^{\infty}V_{n,m} = -2\lambda\sum_{n=0}^{\infty}\sum_{m=0}^{\infty}(l/\sigma + n + m)^{-3} \tag{8}$$

The double summation contains $p + 1$ identical terms for each value of $p = n + m$. Hence,

$$\frac{V}{kT} = -2\lambda\sum_{p=0}^{\infty}(p + 1)(l/\sigma + p)^{-3} \tag{9}$$

For an approximate solution, we consider chains at a large distance ($l \gg \sigma$) and replace (9) by the integral

$$\frac{V}{kT} \approx -2\lambda\int_0^{\infty} dp\,(p + 1)(l/\sigma + p)^{-3} = -2\lambda\left[\frac{1 + l/\sigma}{2(l/\sigma)^2}\right] \tag{10}$$

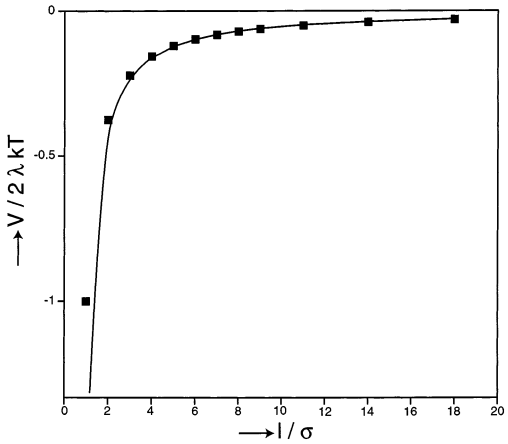

Figure 2. Numerical solution (drawn line) of eq 9 by summing up to $p = 1000$. Squares represent the approximate interaction in eq 10.

Figure 2 shows that eq 10 is a very good approximation of the interaction in eq 9 for $l/\sigma > 2$. Near contact at $l = \sigma$, the approximation is incorrect; the contact energy from eq 9 is actually $V/kT = -2\lambda(1.644)$, instead of -2λ from eq 10. The interaction eq 10 between the chain ends in Figure 1B is mainly determined by the dipoles adjacent to the "gap"; it is less important whether the ends belong to rigid linear chains or to one large ring which closes somewhere outside the box in Figure 1B. Thus eqs 9 and 10 are also relevant for folded chains (see section 4.2). The confinement by the bacteria opposes extensive bending of the chain. However, we expect that once released from bacteria, a chain may close itself to a ring such that all head-to-tail interactions are "saturated". (This is actually the flux-closure ring predicted by Jacobs and Bean[8].) Ring

(13) Lavender, H. B.; Iyer, K. A.; Singer, S. J. *J. Chem. Phys.* **1994**, *101*, 7856.

formation is counteracted by the energy required to bend a chain. For $n \geq 4$ dipoles, rings have a lower potential energy than chains.[13] The difference, however, is small and vanishes for $n \rightarrow \infty$. A ring has no net magnetic moment and is obviously unsuitable for (bacterial) navigation. For this navigation, the energy E of a linear chain of n dipoles (with orientation $\hat{\mathbf{s}}$) in the earth magnetic field $\mathbf{H}$ (with orientation $\hat{\mathbf{s}}_{\mathbf{H}}$),

$$\frac{E}{kT} = -\alpha(\hat{\mathbf{s}}\cdot\hat{\mathbf{s}}_{\mathbf{H}}) \qquad \alpha = \frac{n\mu_0\mu\mathbf{H}}{kT} \tag{11}$$

must be large enough. That is to say, the parameter α must satisfy $\alpha \gg 1$, because otherwise the chain orientation is easily perturbed by thermal or convective motions. Note that the orienting effects of n dipoles in eq 11 simply add up. However, the condition $n \gg 1$ does not necessarily imply that the bacteria have a good "compass". The volume v_p of a magnetite crystal in eq 3 should not be too large to avoid multidomain formation but should neither be too small to avoid thermal instability of the magnetic moment (superparamagnetism) which for magnetite occurs below a radius of roughly 10 nm.

3. Materials and Methods

3.1. Bacterial Cultivation and Preparation. In exploring experiments, we cultivated *Magnetospirillum gryphiswaldense* (DSMZ, Germany). However, these experiments produced bacteria with a minority of only about 5% containing magnetite. Electron microscopy revealed that also in the cells supplied to us by DSMZ the percentage of magnetic bacteria is fairly low. Therefore, we choose to focus on another type of bacteria with a much higher percentage of magnetic cells.

M. magnetotacticum DSM 3856T was cultivated in a gel-like medium following a description in ref 14 which is based on several earlier reports.[3,15,16] Tartaric acid, succinic acid, and sodium acetate are used as a carbon and energy source. The bacteria use ferric quinate for the production of magnetite. Resazurine is used as an indicator for oxygen.

For the growth medium, four different solutions were freshly prepared: a vitamin solution, a trace element solution, a ferric quinate solution, and a resazurine solution. The vitamin solution contained the following vitamins per liter of distilled water: 2.0 mg of biotin (Merck), 2.0 mg of folic acid (Fluka), 10.0 mg of pyridoxine-HCl (OPG Farma), 5.0 mg of thiamin-HCl (Fluka), 5.0 mg of riboflavin (Fluka), 5.0 mg of nicotinic acid (Merck), 5.0 mg of D,L-calcium pantothenate (Sigma), 0.1 mg of vitamin B_{12} (Merck), 5.0 mg of *p*-aminobenzoic acid (Fluka), and 5.0 mg of lipoic acid (Fluka).

The trace element solution contained the following amounts of salts per liter of distilled water: 1.5 g of nitrilotriacetic acid (Fluka), 3.0 g of $MgSO_4\cdot 7H_2O$ (Fluka), 0.5 g of $MnSO_4\cdot 2H_2O$ (Merck), 1.0 g of NaCl (Merck), 0.1 g of $FeSO_4\cdot 7H_2O$ (Merck), 0.18 g of $CoSO_4\cdot 7H_2O$ (Fluka), 0.1 g of $CaCl_2\cdot 2H_2O$ (Merck), 0.18 g of $ZnSO_4\cdot 7H_2O$ (Merck), 0.01 g of $CuSO_4\cdot 5H_2O$ (Merck), 0.02 g of $KAl(SO_4)_2\cdot 12H_2O$ (Merck), 0.01 g of H_3BO_3 (Merck), 0.01 g of $Na_2MoO_4\cdot 2H_2O$ (Merck), 0.025 g of $NiCl_2\cdot 6H_2O$ (Merck), and 0.3 mg of $Na_2SeO_3\cdot 5H_2O$ (Merck).

The 0.01 M ferric quinate solution was prepared by dissolving 0.45 g of $FeCl_3\cdot 6H_2O$ (Fluka) and 1.9 g of quinic acid (Fluka) in 100.0 mL of distilled water. Finally, the resazurine solution was prepared by dissolving 0.1 g of resazurine (Fluka) in 100 mL of distilled water.

The gel-like growth medium consisted of (per 982.5 mL of distilled water) 10.0 mL of vitamin solution, 5.0 mL of trace element solution, 2.0 mL of ferric quinate solution, 0.5 mL of resazurine solution, 0.68 g of KH_2PO_4 (Merck), 0.12 g of $NaNO_3$ (BHD Chemicals Ltd), 0.05 g of sodium thioglycolate (Fluka), 0.37 g of L-(+)-tartaric acid (Merck), 0.37 g of succinic acid (Fluka), 0.05 g of sodium acetate (Acros), and 1.3 g of agar (Difco Laboratories). All chemicals were used as supplied without further purification. The growth medium was prepared by dissolving the components in the order given above. Before addition of the agar, the pH of the medium was adjusted to 6.75 with NaOH. The medium was boiled for 15 min to remove most of the oxygen. Portions of about 40 mL of medium were dispensed in screw-capped 100-mL bottles. The bottles were crimp-sealed with a rubber stopper wired in place, and the atmosphere was replaced by N_2. The bottles were autoclaved at 121 °C for 15 min.

After autoclaving and cooling, sterile oxygen was added to the bottles, a few hours before inoculation, to provide 1% (v/v) O_2 in the gas phase. The media were slightly pink in color. Cells were inoculated into the medium by injection through the stopper. Inocula contained approximately 1 mL (ca. 2×10^8 cells) per 40 mL of medium.

Bacteria were grown at 30 °C. During growth, when the culture became reduced as evidenced by decolorization of the media, a small amount of oxygen and ferric quinate solution was added in order to obtain higher densities of magnetic cells. The cell concentration was determined by microscopic enumeration, using a Bürker-Türk counting chamber.[17]

3.2. Bacterial Cells. Transmission electron microscopy (TEM) was performed with a Philips CM10H electron microscope operating at 80 kV. Samples were prepared by placing Cu grids, coated with a Formvar/carbon film, in a droplet of medium for a few minutes. The grids were dried in air.

Bacteria for elemental analysis were harvested from autoclaved media by centrifugation in a Beckman GS-6 centrifuge for 20 min at 3000 rpm and subsequently washed three times with distilled water. Elemental analysis was performed by induced coupled plasma atomic emission spectrometry (ICP) on a sample of magnetotactic cells, dried at 105 °C to constant weight.

Bacteria for electrophoresis were harvested from freshly autoclaved media by centrifugation in a Beckman GS-6 centrifuge for 20 min at 3000 rpm and subsequently washed three times with distilled water and once with phosphate buffer, pH 7. The 0.05 M phosphate buffer was prepared by dissolving 0.68 g of KH_2PO_4 (Merck) and 0.71 g of Na_2HPO_4 (Merck) in 1 L of distilled water. The electrophoretic mobility of cells in phosphate buffer was determined with a DELSA-440SX instrument (Coulter Electronics, Inc.) from the Doppler shift of scattered light from bacteria moved by the applied electric field.

Bacteria for analytical sedimentation experiments (under gravity) were harvested from freshly autoclaved media by preparative centrifugation in a Beckman GS-6 centrifuge for 20 min at 3000 rpm and subsequently washed three times with distilled water. After the dispersion was centrifuged for the third time, the supernatant was removed and the cell mass was determined by drying a weighted amount of sediment at 105 °C to constant weight. Nine cell suspensions were prepared by dispersing weighted amounts of sediment in phosphate buffer (pH 7) with final concentrations in the range of 0.24−0.48 mg of cells per gram of dispersion. The sedimentation velocity of the cells under gravity was measured with a setup described in detail by Thies-Weesie.[18] The dispersions were poured in glass sedimentation tubes of 1.5 cm diameter and 30 cm length, which were carefully closed. Settling of particles is easily disturbed by even minute vibration or temperature variations.[18] Therefore, the sedimentation tubes were immersed precisely vertically in a water bath on a heavy marble table in a thermostatic room with constant temperature ($T = 21.5 \pm 0.1$ °C). The descent of the dispersion−solvent interface was measured for 70 h. To increase the visibility of the interfaces, the sedimentation tubes were placed in front of a black background. After 70 h, the dispersions were homogenized by shaking and the settling experiment was repeated. Each sample was measured three times, and the resulting sedimentation velocities were averaged.

Magnetization measurements were done with an alternating gradient magnetometer (AGM, MicroMag 2900 of Princeton

(14) Deutsche Sammlung von Mikroorganismen und Zellkulturen (DSMZ, Germany, 1993).

(15) Maratea, D.; Blakemore, R. P. *Int. J. Syst. Bacteriol.* **1981**, *31* (4), 452.

(16) Wolin, E. A.; Wolin, M. J.; Wolfe, R. S. *J. Biol. Chem.* **1963**, *238*, 2882.

(17) Gerhardt, P. *Manual of Methods for General Bacteriology*; American Society for Microbiology: Washington, DC, 1981.

(18) Thies-Weesie, D. M. E.; Philipse, A. P.; Lekkerkerker, H. N. W. *J. Colloid Interface Sci.* **1996**, *177*, 427.

Measurements Corp.). The magnetic moment of a sample was measured as a function of the static magnetic field strength which ranged from −0.5 to 0.5 T. (By applying an alternating field gradient on a magnetized sample, an alternating force is produced which is proportional to the magnetic moment of the sample.) The sample for magnetization measurements was prepared by drying a dispersion of magnetotactic bacteria in distilled water at 105 °C to constant weight. The dried sample was wrapped in Scotch tape and stuck to the sample probe. Further details about sample preparation and analysis can be found in refs 7 and 20.

3.3. Bacterial Magnetite Particles. The first method we used to extract magnetite particles from cells was sonication following Frankel[21] and others.[22,23] Cells dispersed in distilled water were sonicated for 12 min with a Soniprep 150 sonicator at an amplitude of 10 microns. The sonicated samples were centrifuged in a preparative ultracentrifuge (Beckman L-60) for 20 h at 8000 rpm. The magnetite particles were washed three times in distilled water. Magnetic particles were collected at the vessel wall with a bar magnet.

The second method to disrupt cells and collect magnetic particles employs a sodium hydroxide solution following Frankel[21] and Matsunaga.[23] Growth medium with a high cell concentration was poured into a beaker and stirred. Sodium hydroxide platelets were added to the dispersion up to a concentration of 5 M NaOH. After stirring for approximately 16 h, the samples were centrifuged in a preparative ultracentrifuge (Beckman L-60) for 10 h at 8000 rpm. The magnetic particles were washed three times in distilled water and collected with a magnet.

TEM was performed as in section 3.2. The surface area of about 100 particles was measured with an interactive image analysis system to determine the average equivalent sphere diameter.

Elemental analysis was performed by instrumental neutron activation analysis (INAA) on magnetite particles extracted from cells by washing with a sodium hydroxide solution followed by magnetic purification. The sample was dried at 105 °C to constant weight. (INAA was used instead of ICP because the amount of magnetite was insufficient for ICP analysis.)

Magnetization measurements on magnetite particles were performed as in section 3.2. The particles were extracted from cells by washing with a sodium hydroxide solution followed by magnetic purification. The sample was dried to constant weight at 105 °C.

Atomic and magnetic force microscopy imaging was done with a Nanoscope III Dimension 3000 scanning probe (Digital Instruments). The probe consists of a magnetically coated Nanoprobe tip. First, a surface topography image was obtained using the tapping mode, and then a magnetic force image was taken using the liftmode. In the liftmode, the probe is lifted and follows the same height pattern as already measured in the topographical scan. The samples were prepared by drying a droplet of distilled water containing magnetite particles, extracted from cells by washing with a sodium hydroxide solution, on mica platelets.

4. Results and Discussion

4.1. Bacterial Cultivation and Preparation. Inoculation of *M. magnetotacticum* in a gel-like medium in sealed 100-mL bottles produced within a week diffuse, fluffy areas of growth a few centimeters below the medium−air interface. Then the bacteria started to grow upward in the direction of the surface, leading to the reduction of the medium as evidenced by the disappearance of the pink (resazurine) color. By addition of oxygen and ferric quinate during growth, higher densities of magnetic cells were obtained as could be verified by transmission electron microscopy. In about 2 weeks, the population increased from an initial density of about 5×10^6 cells per milliliter to a final concentration of 10^8 to 2×10^8 cells per milliliter. Approximately 70% of the cells produced magnetite particles. Since we managed to cultivate *M. magnetotacticum* on a small scale, we attempted an upscaling to (sealed) 1-L bottles. However, generally the final population density in the 1-L bottles was lower and also the percentage of magnetic cells was much lower than in the 100-mL bottles. Possibly the yield can be improved by keeping the oxygen and ferric quinate concentration and the pH of the medium constant during growth.

4.2. Imaging and Particle Structures. Electron micrographs of *M. magnetotacticum* (grown in 100-mL bottles) are shown in Figure 3. The cell diameter is in the range of 0.2−0.4 μm, and the cell length is 4−6 μm. About 70% of the cells contains magnetite particles, which are aligned in a chain parallel to the long axis of the bacteria. Occasionally also a "branched" chain is observed as shown in Figure 3a. The number of particles in the cells varies from 0 to 45. It is indeed possible to extract magnetite particles from bacterial cells by sonication as well as by washing with a sodium hydroxide solution. Magnetophoresis sometimes is effective to separate the magnetite crystals from organic material (Figure 4), though in other cases a substantial organic residue remains (Figure 4g).

Individual bacterial magnetite particles, which are reported to be cubo-octahedrons,[26] seem to have a somewhat irregular facetted shape. The average surface area of harvested magnetic particles on the TEM pictures is 5.5×10^4 nm^2 with a polydispersity of 24.8%. The mean equivalent sphere diameter is 47.1 nm with a polydispersity of 13.3%. Dimensions of cells and magnetite particles (Tables 1 and 2) are in good agreement with literature values.[3,24−26]

The surface topographic and magnetic force images of dried magnetite particles are shown in Figure 5. The surface topographic force image shows differences in height of the sample surface as measured by the cantilever. The surface topographic image (right) and the magnetic force image (left) show strings of magnetic particles.

The magnetite crystals are single domains with a thermally stable magnetic moment. These magnetic moments are large (λ is about 70, see section 4.6), so when the crystals are confined to lie on a two-dimensional plane (in this case a TEM grid), the moments will orient parallel to the plane such that head-to-tail contacts can be made. The rings in Figure 4c−e are therefore very likely flux-closure rings of in-plane dipoles, possibly the first images of the Jacobs−Bean[8] flux-closure rings for Fe_3O_4 colloids. In conventional magnetite ferrofluids, λ is too small for particles to form such large rings and long chains as in Figure 4c−e. We refer here to a cryo-electron microscopy study[19] on magnetite ferrofluids, in which magnetite particles (typical radius, 5 nm) were shown to have a tendency to form more or less *isotropic* clusters. This tendency was also partly ascribed to the isotropic van der Waals attractions,[19] which may significantly affect the association behavior in a ferrofluid. Since the magnetic attractions increase much faster with particle volume (see eqs 1−3) than van der Waals forces, the latter hardly contribute for suffiently large particles, which is certainly

(19) Donselaar, L.; Frederik, P. M.; Bomans, P.; Buining, P. A.; Humbel, B. M.; Philipse, A. P. *J. Magn. Magn. Mater.* **1999**, *201*, 58.
(20) Instruction manual of MicroMag 2900 Alternating Gradient Magnetometer; Princeton Measurements Corp.: Princeton, NJ, 1993.
(21) Frankel, R. B.; Papaefthymiou, G. C.; Blakemore, R. P.; O'Brien, W. *Biochim. Biophys. Acta* **1983**, *763*, 147.
(22) Denham, C. R.; Blakemore, R. P.; Frankel, R. B. *IEEE Trans. Magn.* **1980**, *16* (5), 1006.
(23) Matsunaga, T.; Tadokoro, F.; Nakamura, N. *IEEE Trans. Magn.* **1990**, *26* (5), 1557.
(24) Schleifer, K. H.; Schuler, D.; Spring, S.; Weizenegger, M.; Amann, R.; Ludwig, W.; Kohler, M. *Syst. Appl. Microbiol.* **1991**, *14*, 379.
(25) Balkwill, D. L.; Maratea, D.; Blakemore, R. P. *J. Bacteriol.* **1980**, *141* (3), 1399.
(26) Mann, S.; Frankel, R. B.; Blakemore, R. P. *Nature* **1984**, *310*, 405.

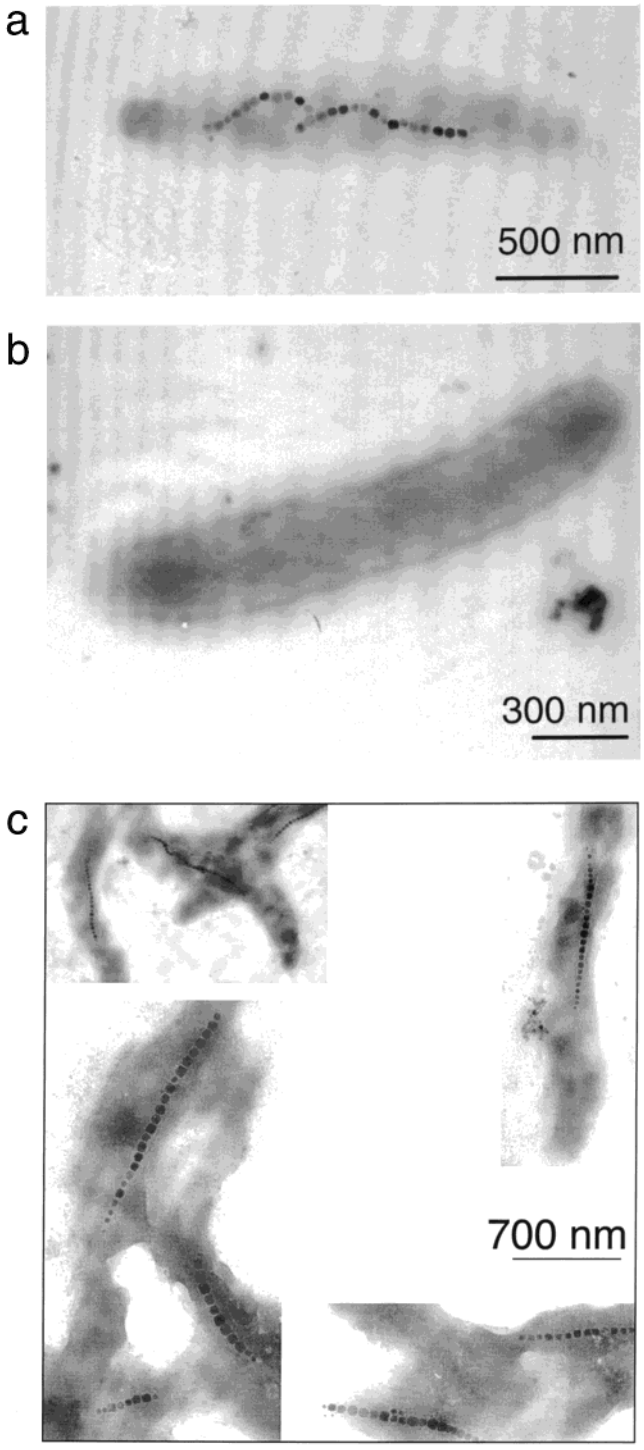

Figure 3. Transmission electron micrographs of (a) a magnetotactic cell (*M. magnetotacticum*, as for all pictures), (b) a nonmagnetotactic cell, and (c) groups of cells with magnetic backbones.

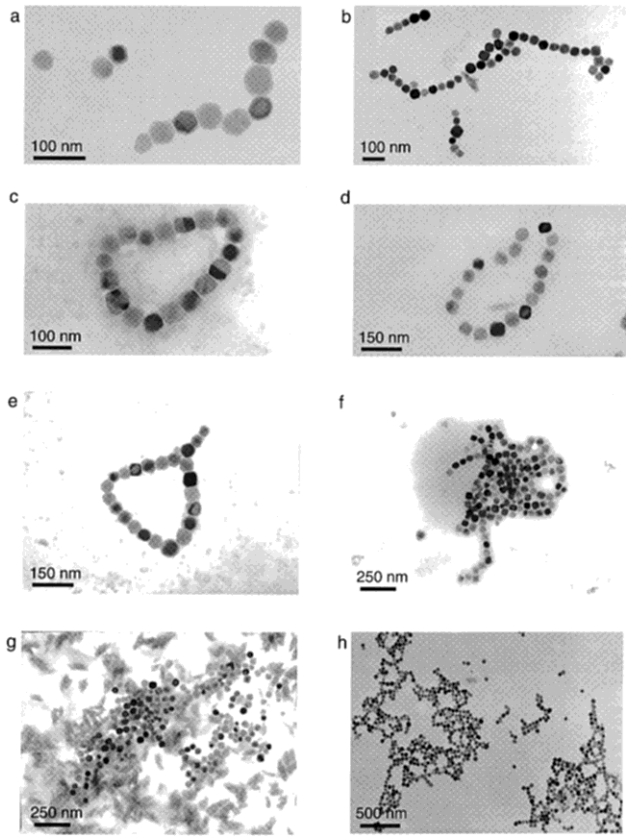

Figure 4. Representative selection of cluster morphologies for magnetite (Fe_3O_4) colloids extracted from cells imaged by transmission electron micrographs. Note the magnetic flux-closure rings in images c, d, and e. The tendency of forming stringlike aggregates can be clearly seen in for example images b and f.

Table 1. Properties of (Dried) Bacterial Cells

length	4−6 μm
diameter	0.2−0.4 μm
fraction magnetotactic cells	70%
number of magnetite particles	0−45
Fe concentration	1.8 mg per gram dry weight
remanent magnetization M_r	2.77 nA/m
coercive field $\mathbf{H}_c$	13.8 mT
maximum magnetization M_s	13.4 nA/m

Table 2. Properties of (Dried) Magnetite Colloids

mean (equivalent) diameter	47.1 nm
polydispersity	13.3%
Fe concentration	9 mg per gram dry weight
remanent magnetization M_r	14.4 nA/m
coercive field $\mathbf{H}_c$	8.13 mT
maximum magnetization M_s	53.9 nA/m

the case for the colloids in Figure 4. The dominance of magnetic attraction is also clearly illustrated by Figure 4d. Here the particles got stuck on the TEM grid at particle surface-to-surface distances up to one particle diameter. Nevertheless, the ring structure has been preserved. Note that breaking a large ring will cost nearly the same dissociation energy as breaking a straight chain. Thus eq 10 can be applied to conclude that for $\lambda \sim 70$ a chain will have a strong tendency to "snap" to a ring already when its ends are still several particle diameters apart. The lowest energy state for a large number of in-plane dipoles is one circular ring. However, deformations easily occur because of screening of dipolar interactions, which weakens the force between opposite ring parts considerably. These shape deformations can be observed in Figure 4c,d.

A peculiar morphology is the "handle"-shaped cluster, an example of which is depicted in Figure 4e. Such handles could be chains, which have folded back unto themselves but not far enough to form a ring. Note that the handle is metastable with respect to a ring, which saturates all dipoles. A handle may also result from the encounter between a closed ring and a linear chain. Figure 4h is an illustrative example of a TEM micrograph of a larger population density of magnetite colloids. A free singlet, as expected for strong dipoles, is a rare event; most particles form aggregates in which strings, deformed rings,

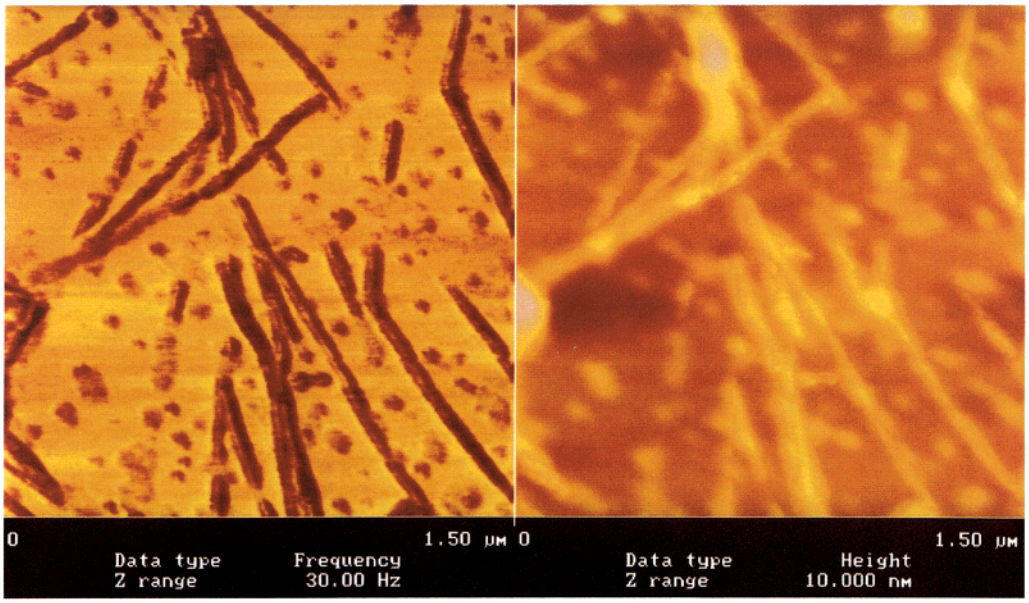

Figure 5. Atomic force microscopy: topographic (right) and magnetic (left) images of magnetic particles extracted from cells.

and handles are present on a local scale involving 10−20 particles. The global image, of course, may be influenced by capillary or shear forces in the preparation of TEM grids. The cluster morphology, nevertheless, resembles simulation snapshots of strongly polar fluids, showing nucleation of dipolar sphere structures which look very similar to Figure 4f.[11]

4.3. Elemental Analysis. The presence of iron in the purified bacteria samples is confirmed by the elemental analysis results. The iron concentration in the bacterial cells, determined with ICP, is about 1.8 mg per gram dry weight. (Blakemore[3] reports in magnetic cells iron concentrations of 20 mg per gram dry weight.) In a small amount of magnetite particles extracted from cells by washing with sodium hydroxide solution, the iron concentration determined with INAA is roughly 9 mg per gram dry weight. In pure magnetite, the iron weight concentration is about 70%; in the sample of magnetite particles extracted from cells, we found a concentration of about 1%. So it can be concluded that magnetite particles extracted from cells and collected with a bar magnet still may contain a relatively large amount of organic material. Part of the organic material may stem from magnetosome membranes around the magnetic particles. Such residues, incidently, are difficult to image with TEM, a technique which is rather insensitive to low-contrast organic material.

4.4. Electrophoresis. The electrophoresis experiments for the bacterial cells in phosphate buffer show that the cell walls carry negative surface charge at neutral pH. The surface charge of the bacteria originates from carboxyl, phosphate, and amino groups. The degree of dissociation of these anionic and cationic groups is determined by the pH and the activity of the surrounding electrolyte solution. Usually bacterial cells are negatively charged at neutral pH, because the number of carboxyl and phosphate groups is generally higher than that of the amino groups.[27]

The ionic strength in our samples is high, so the Debye length is very much smaller than bacterial dimensions. Thus one could attempt to use the classical Helmholtz−Smoluchowski theory[27] for the conversion of the electrophoretic mobility into the ζ-potential, which in our case leads to a ζ-potential of order 1 mV. However, in this theory it is assumed that the ionic atmosphere of the electrical double layer is not deformed by the external electric field. This assumption holds as long as the conduction of ions along or in the particle surface is negligibly small. For bacterial cells, however, surface conduction effects may be considerable, even at low ζ-potentials, depending on the amount of mobile ions in the bacterial wall.[27] Thus for bacterial cells actually no reliable estimate for the magnitude of ζ-potential from electrophoretic mobility can be obtained, unless quantitative information on the cell wall conductivity is available.

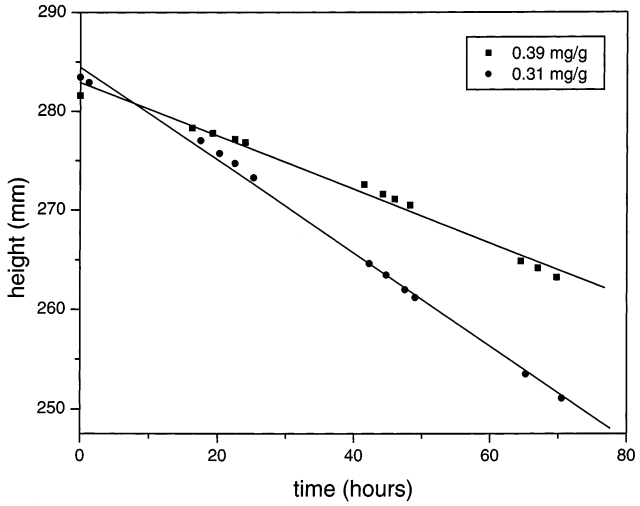

Figure 6. Typical sedimentation results showing the height of the interface between the magnetotactic cells and supernatant (phosphate buffer) versus time, for two bacterial mass concentrations (0.31 and 0.39 mg/g). The solid lines are linear fits.

4.5. Gravitational Sedimentation. During the sedimentation of the magnetotactic cells, a sharp, somewhat bumpy interface was observed between the dispersion and the clear supernatant. In all measurements, the height of the interface descends linearly with time. Figure 6 shows typical results for two mass concentrations. After sedimentation and shaking, the samples showed no flocs or other inhomogeneities indicative of permanent particle coagulation. The bacteria redispersed easily, and the

(27) Wal, A. van der Electrochemical characterization of the bacterial cell surface. Ph.D. Thesis, Wageningen University, Wageningen, The Netherlands, 1996.

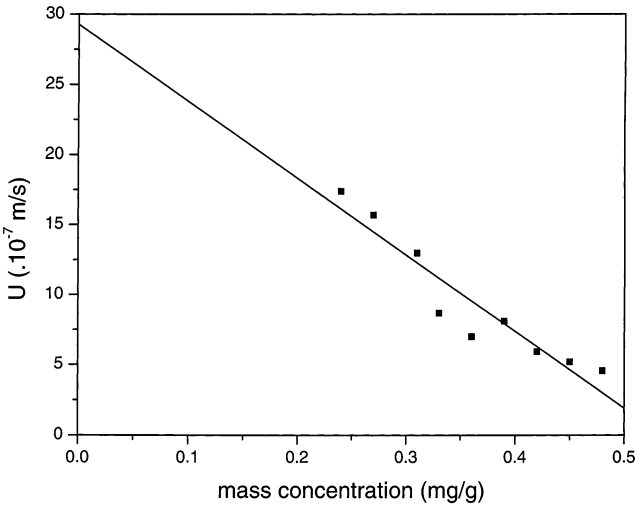

Figure 7. The sedimentation velocities U versus the mass concentration obtained from data as in Figure 7. The solid line is a linear fit.

settling data were reproducible. This reproducibility is a sensitive test for the colloidal stability of the cells, because sedimentation velocities and their reproducibility are very sensitive to even weak attractions or aggregation.[28]

The sedimentation velocity U as a function of the bacterial mass concentration is plotted in Figure 7. The single-bacteria velocity U_0 is found from extrapolation to infinite dilution to be $U_0 = 2.9 \times 10^{-7}$ m s^{-1}. Figure 7 shows that the sedimentation velocity decreases linearly with increasing mass concentration. This linear decrease can be expected for stable colloids with a short-range interparticle repulsion.[29] In a phosphate buffer, the double-layer repulsion between the negative charged bacteria indeed must be of very short range in comparison to the bacteria dimensions. Nevertheless, magnetic or van der Waals attractions due to the iron oxide "backbones" are still masked, because otherwise the sedimentation rate would *increase* with concentration, a well-documented phenomenon for attractive colloids.[29] We note that this positive concentration dependence does not necessarily require permanently aggregated particles. An increased probability for particles to sediment temporarily as a doublet may suffice. The first-order dependence of U on weight concentration c,

$$U = U_0 - kc \tag{12}$$

can be rewritten as

$$\frac{U}{U_0} = 1 - H\varphi \qquad H = k\delta/U_0 \tag{13}$$

for a volume fraction φ of bacteria with mass density δ. For nonspherical colloids, theoretical expressions for H are not available,[29] with the exception of thin, rigid rods. For such rods sedimenting in a random orientation, Dhont recently derived that H varies as[30]

$$H \propto (L/D)^2/\ln(L/D) \qquad \text{for } L/D \gg 1 \tag{14}$$

in which L/D is the rod aspect ratio. Of course, a thin, rigid rod is a poor (hydrodynamic) approximation for bacterial shapes as in Figure 3. However, eqs 13 and 14 confirm the idea that the settling of nonaggregated elongated objects has a negative concentration dependence.

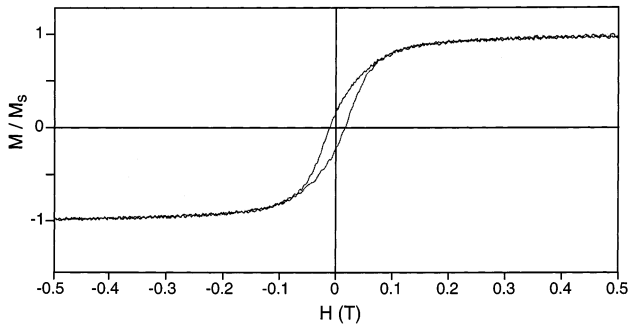

Figure 8. Normalized magnetization M/M_s (M_s is the measured saturation magnetization at high field) of dried magnetite particles extracted from cells versus the applied magnetic field **H**.

4.6. Magnetic Properties. Magnetization measurements with the alternating gradient magnetometer are shown in Figure 8, depicting the normalized magnetization M/M_s versus the applied magnetic field **H** for dried magnetite particles extracted from cells. (For dried bacterial cells, the curves look very similar.) The value of the magnetization at zero field, the remanent magnetization M_r, and the magnitude of the field that must be applied in the negative direction to bring the magnetization back to zero, the coercive field $\mathbf{H}_c$, are given in Tables 1 and 2. These measurements confirm that the magnetite particles produced by the bacterial cells are not superparamagnetic. Whether the magnetic particles are single domain or multidomain cannot be seen in Figure 8. However, for magnetite it is reported that the minimum size at which a particle becomes a multidomain lies between 80 and 120 nm[3]. Bacterial magnetite has a diameter of 47.1 nm, below the critical size for multidomain formation. This is hardly surprising since the chain of magnetic particles will work as a biocompass only if the particles are single domains.

The formation of chains and rings requires that the contact energy between magnetosomes is large. For a bare magnetite sphere with radius $R = 20$ nm, we find, using eq 2, that $\lambda \approx 70$, using the bulk magnetization $m_s \approx 400$ kA/m. This is a substantial attraction, which is not very much weakened if we incorporate the "screening effect" of the lipid layer by a realistic choice of $\Delta = 2$ nm in eq 2, leading to $\lambda \approx 53$.

4.7. Interbacteria Interactions. In our buffer solutions (and in their natural aqueous environment), the Debye screening length is too small to cause any significant electrical double-layer repulsion between the bacteria; there is apparently only a short-range excluded volume repulsion which forbids bacteria to interpenetrate. Then the question arises of why long-range dipole−dipole attractions, strong enough to arrest magnetite particles permanently in a chain with a large total magnetic moment, do not aggregate the bacteria. Indeed, our eq 10 predicts a significant attraction if two magnetite chains would nearly make contact in a head-to-tail configuration as in Figure 1b. Probably such an approach will not be close enough to produce aggregation because usually the bacteria are much longer than their magnetic chains. In a parallel bacteria orientation, however, the chains may be in some instances just a few magnetite diameters apart. Sedimentation results, nevertheless, indicate that side-

(28) Thies-Weesie, D. M. E. Sedimentation and liquid permeation of inorganic colloids. Ph.D. Thesis, Utrecht University, Utrecht, The Netherlands, 1995.
(29) Philipse, A. P. *Curr. Opin. Colloid Interface Sci.* **1997**, *2*, 200.
(30) Dogic, Z.; Philipse, A. P.; Fraden, S.; Dhont, J. K. G. *J. Chem. Phys.* **2000**, *113*, 8368.

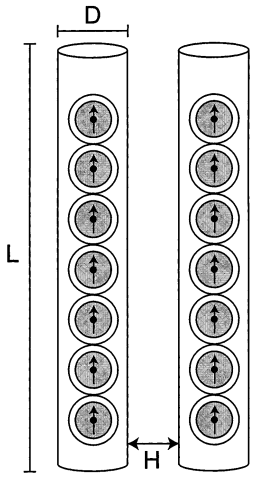

Figure 9. Model used to estimate the attraction between two parallel bacteria due to their magnetite backbones. The dipole chains form the main axis of a nonmagnetic cylindrical shell that determines the distance (D) of closest approach between the dipole centra. H is the surface-to-surface distance of the cylinders.

wise aggregation does not occur. The reason for this stability is very likely the considerable screening of dipolar forces between parallel chains. To quantify this statement, we will model two bacteria as two parallel cylinders with a rigid dipole chain at the main axis. The interaction energy between two parallel, rigid dipole chains of length $L \gg \sigma$ at a distance x (Figure 9) has been calculated by Halsey and Toor.[10] Their result is

$$V/kT = 2\lambda n 4\pi^2(\sigma/x)^{1/2} \exp[-2\pi x/\sigma] \cos(2\pi h/\sigma) \quad (15)$$

where h is the parallel shift of one chain with respect to the other; $L/\sigma = n$ is the number of dipoles in a chain. For $h = z\sigma$ ($z = 0,1,2,...$), the chains repel each other. For $h = (z + {}^1/_2)\sigma$, there is an attraction:

$$V/kT = -2\lambda n 4\pi^2(\sigma/x)^{1/2} \exp[-2\pi x/\sigma] \quad (16)$$

Comparing this result with the dipolar interaction in eqs 1 and 2, we see that the chain−chain attraction is indeed strongly screened. The screening resembles a Yukawa potential with screening length $\sigma/2\pi$. So even for strong intrachain interactions ($\lambda \gg 1$) the interchain interactions are already insignificant at interchain distances of order $x = \sigma$. This implies that parallel magnetotactic bacteria do not experience each other's magnetic backbone. Of course, also van der Waals attractions between the iron oxide chains should be taken into account, because such oxides in water have a large Hamaker constant.[31] We therefore model the total attraction between two magnetite chains as a sum of dipolar forces (eq 16) and van der Waals attractions. We take two chains of 45 magnetite particles with $\sigma = 47$ nm so $L = 2115\ \mu$m and evaluate the interchain attraction using eq 16 (Figure 10). The van der Waals force between the two parallel magnetic cylinders is calculated from the expression of Sparnaay[31,32] using $A = 10^{-19}$ J as an upper estimate of the Hamaker constant for iron oxide in water at room temperature.[31] It turns out

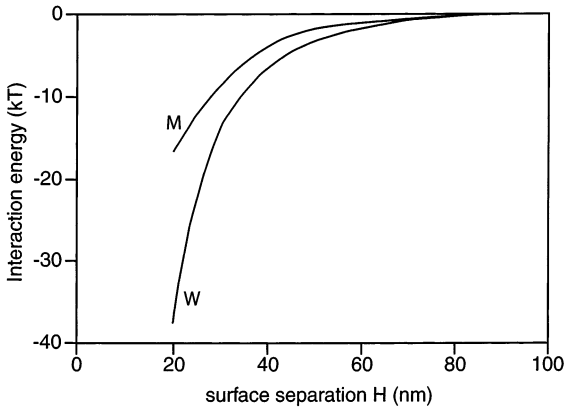

Figure 10. Magnetic attraction (M) and van der Waals attraction (W) between two parallel magnetite chains of length $L = 2.115\ \mu$m and aspect ratio $L/D = 45$.

(Figure 10) that the total attraction (which in our example is actually dominated by the van der Waals force) quickly vanishes for surface-to-surface distances $H = \sigma = 47$ nm. Since a typical bacterial diameter is in the range of 200−400 nm, we can conclude that parallel magnetite chains do not affect the colloidal stability of the bacteria.

65. Conclusions

We have cultivated the magnetotactic bacterium *M. magnetotacticum* on a milligram scale in the laboratory. The negatively charged bacterial cells contain 0−45 magnetite particles, which are aligned in a chain parallel to the longitudinal axis of the cell. The single-domain magnetite colloids harvested from the bacteria form structures such as flux-closure rings of in-plane dipoles and folded chains of the type predicted for colloids with dominant dipolar forces. Such structures clearly resemble the morphologies observed in simulations of strongly dipolar spheres. From sedimentation experiments, we conclude that the net attraction between chains of magnetic particles is too small to produce any aggregation of bacteria. The force between parallel bacterial magnetite backbones is strongly screened, in contrast to the interaction of a single chain with an external field where effects of dipoles add up: the bacteria sense the geomagnetic field but not each other's compass.

Acknowledgment. N. Tan is acknowledged for his explorative study in our group on growth of magnetotactic bacteria. W. Bitter (Molecular Cell Biology, Utrecht University) and C. Pathmamanoharan are thanked for helpful discussions. L. Donselaar, A. George (NMR-spectroscopy, Utrecht University), and A. Ürmenyi are thanked for performing magnetization, sonication, and electrophoresis experiments, respectively. J. Flach (Digital Instruments, Sliedrecht, The Netherlands) performed MAFM measurements. B. J. de Gans and D. Derks contributed to the calculations in section 2. M. Lanen, M. Uit de Bulten, J. den Boesterd, and I. van Rooyen are thanked for their help in preparing the manuscript. A.P. recalls with pleasure discussions with J. Moonen on animal navigation. Part of the investigation was supported by The Netherlands Foundation for Chemical research (SON) with financial aid from The Netherlands Organization for Scientific Research (NWO).

LA0205811

(31) Lyklema, J. *Fundamentals of Colloid And Interface Science*; Academic Press: London, 1993; Vol. I.
(32) Sparnaay, M. J. *Recl. Trav. Chim.* **1959**, *78*, 680.